Pergamon

Int. J. Heat Mass Transfer. Vol. 39, No. 6, pp. 1235–1241, 1996

0017–9310/96 $15.00+0.00

0017–9310(95)00194–8

Temperature and soot concentration in a high soot density flame

M. A. AL-NIMR
Mechanical Engineering Department, Jordan University of Science and Technology, Irbid, Jordan

V. S. ARPACI
Department of Mechanical Engineering and Applied Mechanics, The University of Michigan, Ann Arbor, MI 48109, U.S.A.

and

Y. S. NAJJAR
Mechanical Engineering Department, King Abdul Aziz University, Jeddah, Saudi Arabia

(*Received* 20 *September* 1994 *and in final form* 26 *May* 1995)

Abstract—The emissivity of a particulate flame which contains interacting soot particles of size parameters larger than Rayleigh limit and up to Penndorf extension is derived. The flame is assumed to be heavily charged with soot particles and radiation from the flame is mainly dominated by that emitted or absorbed by particles. It is found that interaction mechanisms have no significant effects on the emissivity of the flame. However, for flames containing soot particles of large size parameters, the emissivity deviates considerably from that estimated based on the Rayleigh limit assumption. Also, a modified version of the monochromatic Schmidt method is proposed to predict the temperature and soot concentration of flames which contain interacting soot particles having size parameters larger than Rayleigh limit and up to Penndorf extension.

INTRODUCTION

Thermal radiation from particulate-laden media plays an important role in combustion systems. Examples are oil and gas-fired furnaces, pulverized coal combustion, radiative burners, solid propellant rockets, gas turbine combustors, internal combustion engines and natural fires. The use of heavier fuels or rich fuel–air ratio in these examples increases the soot formation rate, especially in the primary zone of the combustion system. As a result, radiation from the flame increases, and is dominated mainly by that emitted or absorbed by soot particles. It is important for the designer of a combustion system to predict soot formation on a quantitative basis, rather than from the limited data which can be inferred from exhaust smoke measurements. To achieve a quantitative prediction, the flame temperature and its soot concentration need to be determined. In the literature, three measurement techniques are available [1]. The first technique is to sample the combustion gas and then determine the extracted soot by electron microscopy. The second technique is based on light scattering where incident light is directed to the flame and then scattered radiation is detected. The third technique which is suggested by Schmidt and used in variant forms [2] involves radiation measurements from the flame with hot and cold backgrounds and radiation measurements from the hot background alone. This technique assumes that soot acts primarily to absorb radiation and not to scatter it. This is true for Rayleigh particles which have a small size parameter. An alternative measurement technique requires the knowledge of the spectral coefficients. These coefficients for a single particle can be obtained from the classical Lorenz–Mie (LM) theory for isotropic and homogeneous spherical particles [3, 4] or from its limit, the Rayleigh approximation [5] or the Penndorf extension [6].

For a cloud containing a relatively small number of soot particles, each particle in the cloud acts independently in the absorption and scattering of radiation, and is unaffected by the presence of other particles. The radiative properties of the cloud are then obtained by algebraically adding the properties of each isolated particle. However, when the cloud is heavily charged with particles, the assumption of independent scattering and absorption breaks down due to two fundamental mechanisms [7, 8]. The first mechanism is the near-field interparticle effect, where the internal field of each particle is affected by the presence of the others. Consequently this modifies the amount of radiation absorbed as well as the amount of radiation scattered by each particle. The second is that of coherent addition of the scattered radiation by

NOMENCLATURE

C_1	first radiation constant
C_2	second radiation constant
D	diameter of the particle
$E_{b\lambda}$	emissive power of black body
f_v	solid volume fraction
h_1	parameter appears in the definition of ξ and related to the mechanical interaction among particles
i	complex unit
I	'the imaginary part of'
k	absorptive index
L	mean beam length
LM	Lorenz–Mie theory
m	complex refractive index, $n+ik$
n	refractive index
N	particle number density
P	normalized size distribution function
Q_a, Q_e and Q_s	absorption, extinction and scattering efficiency factors, respectively
R_e	'real part of'
$R_{1,\lambda}$	monochromatic emissive power of the flame with a cold, non-reflecting background
$R_{2,\lambda}$	monochromatic emissive power of the flame with a hot black body background
$R_{3,\lambda}$	monochromatic emissive power of the black body background
T	temperature
$\mathbf{X}_M$	scattering matrix estimated from LM theory.

Greek symbols

α	size parameter, $\pi D/\lambda$
α_m	mean size parameter, $\pi D/\lambda_m$
α	absorbtivity
γ	far-field correction factor
γ_0, γ_1	parameters appear in the definition of γ and depend on the type of mechanical interaction among particles
ε	the emissivity of the flame
ε	relative dielectric constant [m^2]
Σ	Stefan–Boltzmann constant
ξ	complex correction factor depends on the type of mechanical interaction
λ	wavelength
λ_m	mean wavelength
$\psi^{(3)}$	pentagamma function.

Subscripts

a	absorption
b	black body
D	dependent effect
e	extinction
f	flame
I	independent assumption
M	Mie theory for one particle
N	N particles
s	scattering
λ	monochromatic properties.

Superscripts

P	Penndorf limit
R	Rayleigh limit.

each particle in the far field which is manifested by a change in the total scattered field.

The present work is aimed at the prediction of soot concentration and temperature of a heavily charged flame. To attain this goal, the emissivity of a particulate flame, which contains interacting soot particles and other radiation properties, is derived. The study extends the investigation to particles having size parameters up to the Penndorf limit. Also, a modified version of the monochromatic Schmidt method is suggested to predict the soot concentration and temperature of the flame. The proposed method, called the two-distinct wavelengths approach, involves two radiation measurements, instead of three required by other classical methods. These radiation measurements are taken at two distinct wavelengths from the flame with a cold background.

ANALYSIS

For a given particle in a dense particulate system, the scattering, extinction and absorption efficiency factors are [7]

$$Q_{sD} = |\xi|^2 \gamma Q_{sM} \tag{1}$$

$$Q_{eD} = \frac{4}{\alpha^2} Re[\xi \mathbf{X}_M \cdot \mathbf{e}_x|_{\theta=0}] \tag{2}$$

$$Q_{aD} = Q_{eD} - Q_{sD} \tag{3}$$

where subscript D refers to the effect of interaction among particles on the properties, M refers to the properties of non-interacting particles evaluated using LM theory, $\alpha = \pi D/\lambda$ is the size parameter; λ being the wavelength of the incident radiation, D the diameter of the spherical particle, and $\mathbf{X}_M$ is the scattering matrix for a single particle based on the LM theory. Also, ξ is the near-field correction factor which modifies the internal field of each particle due to its enhancement by the presence of other particles, and γ is the far-field correction factor which accounts for the coherent addition of the scattered radiation. In equations (1) and (2), the particles satisfy the Rayleigh–Debye scattering condition: $2\alpha|m-1| \ll 1$, where m is the complex refractive index of the particle. For non-interacting particles, Q_{sM} and $\mathbf{X}_M \cdot \mathbf{e}_x|_{\theta=0}$ are derived by the LM theory in terms of an infinite series. Penndorf [6] obtained expressions for these terms in which α^7 and higher order terms are truncated in $\mathbf{X}_M \cdot \mathbf{e}_x|_{\theta=0}$ and in which α^8 and higher order terms are truncated in Q_{sM}. These expressions are [9]

$$Q^P_{sM} = \tfrac{8}{3}\alpha^4\left|\frac{\varepsilon-1}{\varepsilon+2}\right|^2\left[1+\frac{2\alpha^2}{N_1^2+(2+N_2)^2}\times\left(\tfrac{3}{5}(N_3-4)-2N_1\alpha\right)\right] \quad (4)$$

$$\mathbf{X}_M \cdot \mathbf{e}_x|_{\theta=0} = -i\alpha^3\left(\frac{\varepsilon-1}{\varepsilon+2}\right)\left[1+\frac{\alpha^2}{15}\left(\frac{\varepsilon-1}{\varepsilon+2}\right)\times\left(\frac{\varepsilon^2+27\varepsilon+38}{2\varepsilon+3}-1\right)\right]+\frac{2\alpha^6}{3}\left[\frac{\varepsilon-1}{\varepsilon+2}\right]^2 \quad (5)$$

where $\varepsilon = m^2$, $m = n+ik$, $N_1 = 2nk$, $N_2 = n^2-k^2$ and $N_3 = N_1^2+N_2^2$.

The near-field complex correction factor ξ is [7]

$$\xi = \left[1-\frac{\varepsilon-1}{\varepsilon+2}f_v(1+h_1\alpha^2)\right]^{-1} \quad (6)$$

where f_v is the particles volume fraction $= N\pi D^3/6$, N is the number of particles per unit volume and h_1 has values depending on the statistical model used to describe the mechanical interaction among particles. Equation (6) is expanded as

$$\xi = A_1+A_2\alpha^2+A_3\alpha^4+(B_1+B_2\alpha^2+B_3\alpha^4)i \quad (7)$$

where

$$A_1 = 1+W_1 f_v+f_v^2(W_1^2-W_2^2)$$
$$A_2 = W_1 f_v h_1+2h_1 f_v^2(W_1^2-W_2^2)$$
$$A_3 = h_1^2 f_v^2(W_1^2-W_2^2)$$
$$B_1 = W_2 f_v+2f_v^2 W_1 W_2$$
$$B_2 = W_2 f_v h_1+4h_1 f_v^2 W_1 W_2$$
$$B_3 = 2h_1^2 f_v^2 W_1 W_2$$
$$W_1 = \frac{(N_2-1)(N_2+2)+N_1^2}{(N_2+2)^2+N_1^2}$$
$$W_2 = \frac{3N_1}{(N_2+2)^2+N_1^2}$$
$$W_3 = \frac{T_1T_2+2N_1T_3}{T_4}$$
$$W_4 = \frac{T_2T_3-2N_1T_1}{T_4}$$
$$T_1 = N_2^2-N_1^2+27N_2+38$$
$$T_2 = 2N_2+3 \quad T_3 = 2N_1N_2+27N_1$$
$$T_4 = (2N_2+3)^2+4N_1^2.$$

Also, equation (5) is expanded as

$$\mathbf{X}_M \cdot \mathbf{e}_x|_{\theta=0} = (S_1\alpha^3+S_2\alpha^5+S_3\alpha^6)i+(V_1\alpha^3+V_2\alpha^5+V_3\alpha^6) \quad (8)$$

where

$$S_1 = -W_1 \quad S_2 = -\frac{W_1}{15}(W_1W_3-W_2W_4)+\frac{W_2}{15}(W_1W_4+W_2W_3) \quad S_3 = \tfrac{4}{3}W_1W_2$$

$$V_1 = W_2 \quad V_2 = \frac{W_2}{15}(W_1W_3-W_2W_4)+\frac{W_1}{15}(W_1W_4+W_2W_3) \quad V_3 = \tfrac{2}{3}(W_1^2-W_2^2).$$

A combination of equations (7) and (8) yields

$$(\xi\mathbf{X}_M \cdot \mathbf{e}_x|_{\theta=0}) = \bar{Y}_1\alpha^3+\bar{Y}_2\alpha^5+\bar{Y}_3\alpha^6+(\bar{Z}_1\alpha^3+\bar{Z}_2\alpha^5+\bar{Z}_3\alpha^6)i \quad (9)$$

where

$$\bar{Y}_1 = A_1V_1-B_1S_1$$
$$\bar{Y}_2 = A_1V_2-B_1S_2+A_2V_1-B_2S_1$$
$$\bar{Y}_3 = A_1V_3-B_1S_3$$
$$\bar{Z}_1 = A_1S_1+B_1V_1$$
$$\bar{Z}_2 = B_1V_2+A_2S_1+B_2V_1+A_1S_2$$
$$\bar{Z}_3 = A_1S_3+B_1V_3.$$

Now, from equation (2), the extinction efficiency factor for interacting Penndorf particles is

$$Q^P_{eD} = Y_1\alpha+Y_2\alpha^3+Y_3\alpha^4 \quad (10)$$

where

$$Y_1 = 4\bar{Y}_1 \quad Y_2 = 4\bar{Y}_2 \quad Y_3 = 4\bar{Y}_3.$$

The first term in equation (10) represents the extinction efficiency factor for interacting Rayleigh particles. The deviation of the extinction factor for Penndorf interacting particles from that for Rayleigh interacting particles is shown in Fig. 1. As is clear from this

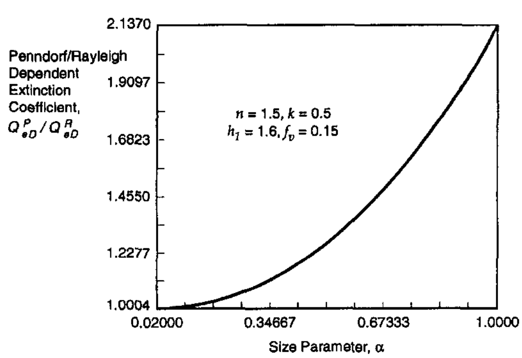

Fig. 1. The deviation of Penndorf extinction factor from Rayleigh extinction factor vs size parameter.

figure, the deviation reaches a value of 113% at size parameter $\alpha = 1$.

To get an expression for $Q^{\mathrm{P}}_{\mathrm{sD}}$, the far field correction factor γ needs to be specified. This factor is [7]

$$\gamma = \gamma_0 + \gamma_1 \alpha^2 \tag{11}$$

where the values of γ_0 and γ_1 depend on f_v and on the statistical model used to describe the mechanical interaction among particles. The scattering efficiency factor for interacting particles is given by inserting equations (4), (7) and (11) into equation (1) to yield

$$Q^{\mathrm{P}}_{\mathrm{sD}} = P_1\alpha^4 + P_2\alpha^6 + P_3\alpha^7 \tag{12}$$

where

$$P_1 = \frac{8\gamma_0}{3}(W_1^2 + W_2^2)$$

$$P_2 = \tfrac{8}{3}(W_1^2 + W_2^2)\left(\frac{6M_2\gamma_0}{5M_1} + \gamma_1\right)$$

$$P_3 = \frac{32N_1\gamma_0}{3M_1}(W_1^2 + W_2^2)$$

$$M_1 = N_1^2 + (2+N_2)^2 \quad M_2 = N_3 - 4.$$

The absorption efficiency factor is given in terms of equations (3), (10) and (12) as

$$Q^{\mathrm{P}}_{\mathrm{aD}} = Y_1\alpha + Y_2\alpha^3 + (Y_3 - P_1)\alpha^4 - P_2\alpha^6 - P_3\alpha^7 \tag{13}$$

where the first term,

$$Q^{\mathrm{R}}_{\mathrm{aD}} = Y_1\alpha \tag{14}$$

is the absorption efficiency factor for interacting Rayleigh particles. For non-interacting particles,

$$Y_1 = \frac{12N_1}{(N_2+2)^2 + N_1^2}$$

and as a result the absorption efficiency factor is reduced to [13]

$$Q^{\mathrm{R}}_{\mathrm{aI}} = \frac{12N_1\alpha}{(N_2+2)^2 + N_1^2}. \tag{15}$$

The deviation of the monochromatic absorption efficiency factor for non-interacting Rayleigh particles from that for interacting particles is shown in Fig. 2.

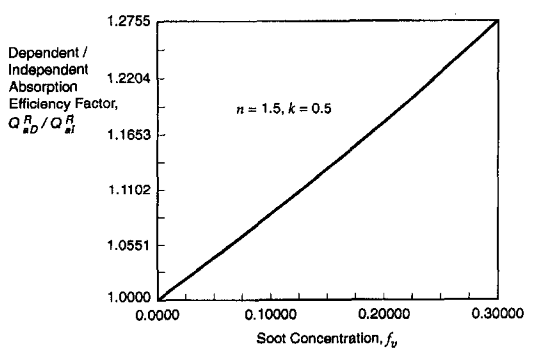

Fig. 2. The ratio of dependent to independent absorption efficiency factor vs soot concentration.

According to this figure, interaction effects become significant when $f_v > 0.1$.

Emissivity of a sooty flame

To predict the temperature and soot concentration of the flame, the flame monochromatic and total emissivity need to be found. From definition, the emissivity of a sooty flame is defined as

$$\varepsilon_{\mathrm{f},\lambda} = 1 - \mathrm{e}^{-\kappa_{\mathrm{a},\lambda}L} \tag{16}$$

where L is an appropriate average length (the mean beam length) which is in general a function of the geometry and $\kappa_{\mathrm{a},\lambda}$ is the spectral absorption coefficient,

$$\kappa_{\mathrm{a},\lambda} = \int_0^\infty Q_{\mathrm{a,D}}\frac{\pi}{4}D^2NP(D)\,\mathrm{d}D \tag{17}$$

where $P(D)$ is the normalized particle size distribution function,

$$\int_0^\infty P(D)\,\mathrm{d}D = 1. \tag{18}$$

For a monodisperse medium, equation (17) is integrated in terms of equation (13) to yield

$$\kappa^{\mathrm{P}}_{\mathrm{a},\lambda,\mathrm{D}} = \frac{3f_v}{2D}[Y_1\alpha + Y_2\alpha^3 + (Y_3 - P_1)\alpha^4 - P_2\alpha^6 - P_3\alpha^7] \tag{19}$$

where the first term $(3f_vY_1\alpha)/(2D)$ is the monochromatic absorption coefficient for interacting Rayleigh particles. Now, the monochromatic emissivity of a flame which contains interacting Penndorf particles is given in terms of equations (16) and (19) as

$$\varepsilon^{\mathrm{P}}_{\mathrm{f},\lambda,\mathrm{D}} = 1 - \mathrm{e}^{-\frac{3f_v}{2}[Y_1\alpha + Y_2\alpha^3 + (Y_3 - P_1)\alpha^4 - P_2\alpha^6 - P_3\alpha^7]\frac{L}{D}} \tag{20}$$

and the monochromatic emissivity of a flame which contains interacting Rayleigh particles is given as

$$\varepsilon^{\mathrm{R}}_{\mathrm{f},\lambda,\mathrm{D}} = 1 - \mathrm{e}^{-\frac{3f_v}{2}Y_1\alpha\frac{L}{D}}. \tag{21}$$

For non-interacting Penndorf particles, the monochromatic emissivity of the flame is still described by equation (20) but with

$$Y_1 = 4V_1 \quad Y_2 = 4V_2 \quad Y_3 = 4V_3$$

$$P_1 = \tfrac{8}{3}(W_1^2 + W_2^2) \quad P_2 = \tfrac{8}{3}(W_1^2 + W_2^2)\left(\frac{6M_2}{5M_1}\right)$$

$$P_3 = \frac{32N_1}{3M_1}(W_1^2 + W_2^2).$$

The variation of monochromatic emissivity with f_v for interacting and non-interacting particles is shown

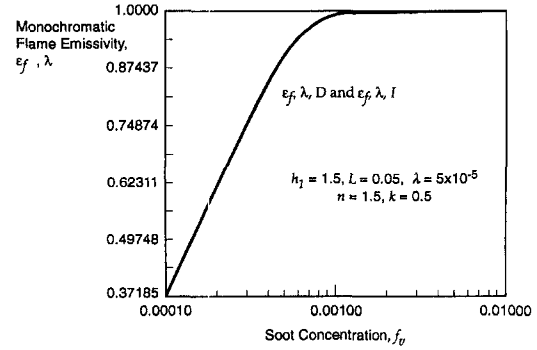

Fig. 3. The variation of monochromatic emissivity of flames containing interacting and non-interacting particles with soot concentration.

in Fig. 3. As is apparent from this figure, interaction mechanisms have no significant effects on $\varepsilon_{f,\lambda}$. In fact, interaction effects are predicted to appear when $f_v > 0.1$ [7]. However, over this range, particulate flames behave like a blackbody which has $\varepsilon_{f,\lambda} = 1$. Also, the deviation of the monochromatic flame emissivity based on Rayleigh limit assumption from that based on Penndorf extension is shown in Fig. 4 for one refractive index typical for soot. The figure clearly demonstrates the importance of the Penndorf correction on the Rayleigh limit by plotting the error in the Rayleigh emissivity vs size parameter α. This error is defined as

$$\text{Error} = \left|\frac{\varepsilon^{P}_{f,\lambda} - \varepsilon^{R}_{f,\lambda}}{\varepsilon^{P}_{f,\lambda}}\right|. \qquad (22)$$

Now, the total emissivity for an isothermal medium is defined as

$$\varepsilon = 1 - \frac{\int_0^\infty E_{b,\lambda}\, e^{-\kappa_{a,\lambda} L}\, d\lambda}{\sigma T^4}. \qquad (23)$$

Here $E_{b,\lambda}$ is the Planck's distribution expressed as

$$E_{b\lambda} = \frac{C_1}{\lambda^5 [e^{[C_2/(\lambda T)]} - 1]} \qquad (24)$$

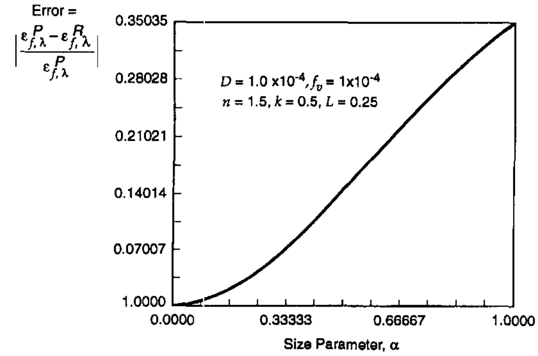

Fig. 4. The deviation of monochromatic emissivity for flame containing Rayleigh particles from that containing Penndorf particles.

where C_1 and C_2 are the first and the second radiation constants, respectively.

The total emissivity for a flame containing interacting Rayleigh particles is given in terms of equations (21) and (23) as

$$\varepsilon^{R}_{f,D} = 1 - \frac{15}{\pi^4}\Psi^{(3)}\left(1 + \frac{3\pi f_v Y_1 L T}{2C_2}\right) \qquad (25)$$

where $\Psi^{(3)}$ is the pentagamma function [10]. A simplified form for the total emissivity of Rayleigh interacting particles may be obtained if equation (23) is integrated using Wien's approximation for $E_{b,\lambda} (= C_1 \lambda^{-5} \exp^{-C_2/\lambda T})$. This approximation yields

$$\varepsilon^{R}_{f,D} = 1 - \frac{1}{\left(1 + \frac{3\pi f_v Y_1 L T}{2C_2}\right)^4}. \qquad (26)$$

An exact, closed form expression for the total emissivity of a flame containing Penndorf interacting particles does not appear to be feasible. However, the substitution of the emission mean wavelength λ_m into equation (20) gives approximate values for $\varepsilon^{P}_{f,D}$ [1]. The mean wavelength is defined as the wavelength which splits the distribution of radiation emitted by a black body to two equal parts and is [11]

$$\lambda_m = \frac{0.004110}{T}. \qquad (27)$$

Now, by substituting λ_m for λ in equation (20), the total emissivity for flame of Penndorf interacting particles is given as

$$\varepsilon^{P}_{f,D} = 1 - e^{\left\{-\frac{3f_v}{2}[Y_1\alpha_m + Y_2\alpha_m^3 + (Y_3 - P_1)\alpha_m^4 - P_2\alpha_m^6 - P_3\alpha_m^7]\frac{L}{D}\right\}} \qquad (28)$$

where $\alpha_m = \pi D/\lambda_m$. For flames containing interacting Rayleigh soot particles, equation (28) is reduced to

$$\varepsilon^{R}_{f,D} = 1 - e^{\left\{-\frac{3f_v}{2} Y_1 \alpha_m \frac{L}{D}\right\}}. \qquad (29)$$

In the following section, the approaches usually used to predict temperature and soot concentration in flames that contain non-interacting Rayleigh particles are extended to include both interaction effects and larger size parameter limits (Penndorf extension).

RADIATION MEASUREMENT METHODS—MONOCHROMATIC SCHMIDT METHOD

This method was originally suggested by Schmidt [11] to predict the characteristics of gray flames. However, the method may be used monochromatically for a precise prediction [2]. The monochromatic Schmidt method requires three readings, which are:

(a) $R_{1,\lambda}$ = monochromatic emissive power of the flame with a cold, non-reflecting background.

(b) $R_{2,\lambda}$ = monochromatic emissive power of the flame with a hot black body background.

(c) $R_{3,\lambda}$ = monochromatic emissive power of the black body background without flame.

These three readings are expressed in terms of Planck's law for black body radiation as,

$$R_{1,\lambda} = \varepsilon_{f,\lambda} E_{b,\lambda}(T_f) \tag{30}$$

$$R_{2,\lambda} = \varepsilon_{f,\lambda} E_{b,\lambda}(T_f) + (1-\alpha_{f,\lambda}) E_{b,\lambda}(T_B) \tag{31}$$

$$R_{3,\lambda} = E_{b,\lambda}(T_B) \tag{32}$$

where T_B is the hot black body temperature and $\alpha_{f,\lambda}$ is the monochromatic flame absorptivity. Substituting equations (30) and (32) into equation (31) gives

$$R_{2,\lambda} = R_{1,\lambda} + (1-\alpha_{f,\lambda}) R_{3,\lambda}. \tag{33}$$

This equation is solved for $\alpha_{f,\lambda}$ to give

$$\alpha_{f,\lambda} = 1 - \frac{R_{2,\lambda} - R_{1,\lambda}}{R_{3,\lambda}}. \tag{34}$$

Now, according to Kirchhoff's law, the spectral flame absorptivity $\alpha_{f,\lambda}$ is equal to the spectral flame emissivity $\varepsilon_{f,\lambda}$ for diffuse flames. Thus,

$$\varepsilon_{f,\lambda} = 1 - \frac{R_{2,\lambda} - R_{1,\lambda}}{R_{3,\lambda}}. \tag{35}$$

Now, for flames that contain interacting Penndorf particles, the temperature of the flame is given from equation (30) as

$$T_f = \frac{C_2}{\lambda \ln\left[1 + \dfrac{C_1 \varepsilon_{f,\lambda}}{\lambda^5 R_{1,\lambda}}\right]}. \tag{36}$$

Also, the concentration of soot particles within Penndorf limit may be found from equation (20) as

$$f_v^P = -\frac{D \ln(1-\varepsilon_{f,\lambda})}{\frac{3}{2} L [Y_1 \alpha + Y_2 \alpha^3 + (Y_3 - P_1)\alpha^4 - P_2 \alpha^6 - P_3 \alpha^7]}. \tag{37}$$

For particles within Rayleigh limit, equation (37) is reduced to

$$f_v^R = -\frac{D \ln(1-\varepsilon_{f,\lambda})}{\frac{3}{2} L Y_1 \alpha} \tag{38}$$

where $\varepsilon_{f,\lambda}$ is the flame emissivity estimated from radiation measurements as given in equation (35). The right-hand sides of equations (37) and (38) are functions of f_v and, as a result, these equations have to be solved numerically for f_v. However, as mentioned previously, interaction has no significant effect on $\varepsilon_{f,\lambda}$ and soot particles may be assumed to behave independently. Accordingly, the dependence of the right-hand sides of equations (37) and (38) on f_v vanishes. For this case, the volume fraction ratio of non-interacting Penndorf particles to that of non-interacting Rayleigh particles is

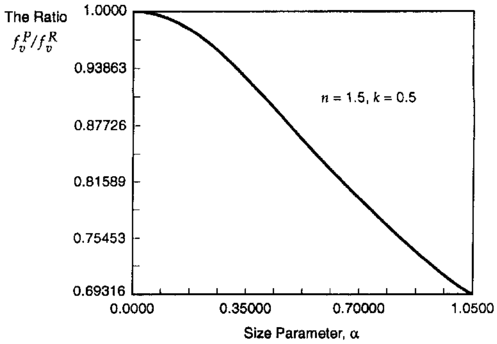

Fig. 5. The deviation of soot concentration estimated for Penndorf particles from that estimated for Rayleigh particles.

$$\frac{f_v^P}{f_v^R} = \frac{1}{1 + \dfrac{Y_2}{Y_1}\alpha^2 + \dfrac{(Y_3 - P_1)}{Y_1}\alpha^3} \tag{39}$$

where terms of order α^5 and higher are neglected and

$$Y_1 = 4V_1 \quad Y_2 = 4V_2 \quad Y_3 = 4V_3$$

$$P_1 = \tfrac{8}{3}(W_1^2 + W_2^2).$$

The deviation of f_v^P from f_v^R with size parameter is shown in Fig. 5. As is clear from this figure, the ratio f_v^P/f_v^R reaches a value of 0.7 at $\alpha = 1.0$ which remains within the limit of Penndorf extension. In the following section, a two-distinct wavelengths approach is proposed which predicts both soot concentration and temperature of a sooty flame.

TWO-DISTINCT WAVELENGTHS APPROACH

The Schmidt method requires three radiation measurements to predict the temperature and soot concentration in the flame. These measurements need to be conducted for three different arrangements of the flame and its background. Here, a simpler approach is proposed. The approach requires two radiation measurements conducted at two distinct wavelengths from the flame with cold, non-reflecting background and for only one arrangement of the flame and its background. The required readings by the proposed method are

$$R_{1,\lambda 1} = \varepsilon_{f,\lambda 1} E_{b,\lambda 1}(T_f) \tag{40}$$

$$R_{1,\lambda 2} = \varepsilon_{f,\lambda 2} E_{b,\lambda 2}(T_f). \tag{41}$$

Now, in terms of Wien's approximation for $E_{b,\lambda}$ and the monochromatic emissivity as given by equation (20), the flame temperature is eliminated by combining equations (20), (40) and (41) to yield

$$\frac{\varepsilon_{f,\lambda 1}}{(\varepsilon_{f,\lambda 2})^{\lambda_2/\lambda_1}} = \frac{R_{1,\lambda 1}}{(R_{1,\lambda 2})^{\alpha_1/\alpha_2}} C_1^{(\alpha_1-\alpha_2)/\alpha_2} (\pi D)^{5(1-(\alpha_1/\alpha_2))} \frac{\alpha_2^{5(\alpha_1/\alpha_2)}}{\alpha_1^5}$$

$$= \frac{1-e^{-\frac{3f_v}{2}[Y_1\alpha_1+Y_2\alpha_1^3+(Y_3-P_1)\alpha_1^4-P_2\alpha_1^6-P_3\alpha_1^7]\frac{L}{D}}}{\left[1-e^{-\frac{3f_v}{2}[Y_1\alpha_2+Y_2\alpha_2^3+(Y_3-P_1)\alpha_2^4-P_2\alpha_2^6-P_3\alpha_2^7]\frac{L}{D}}\right]^{\alpha_1/\alpha_2}} \tag{42}$$

where $\alpha_1 = \pi D/\lambda_1$ and $\alpha_2 = \pi D/\lambda_2$. Equation (42) needs to be solved numerically, in terms of the measured values $R_{1,\lambda 1}$ and $R_{1,\lambda 2}$, to find the soot concentration f_v. The flame temperature may be found using equation (40) to yield

$$T_f = \frac{C_2}{\lambda_1 \ln\left[\frac{\varepsilon_{f,\lambda 1} C_1}{R_{1,\lambda 1}\lambda_1^5}\right]}. \tag{43}$$

Measurement techniques which require two radiation readings, and similar to the proposed two-distinct wavelengths method, are available in the literature [12]. However, these methods assume the readings to be taken under different arrangements for the flame and its background. An example for these two-measurement methods is the two-path method [11]. This method involves the use of a mirror as a background and requires two radiation readings which are the radiation from the flame itself, and the radiation from the flame plus that which has been reflected from the mirror and attenuated by the flame. Clearly, the two-path method requires two different arrangements for the flame; these are the flame alone and the flame with a mirror as a background. On the other hand, the two-distinct wavelengths method requires one arrangement for the flame with a cold background. Also, the proposed two-distinct wavelengths method is similar to the two-colour method which is used to predict the temperature of a given surface which has unknown emissivity. However, the two-colour method, in its original form, cannot be used to predict the flame temperature because the radiation pyrometer receives radiation not only from the flame, but also from the background.

CONCLUDING REMARKS

In this work the emissivity of a sooty flame, which is heavily charged with soot particles, has been derived where both interaction and size parameters effects have been considered. It is found that interaction mechanisms have no significant effects on the emissivity. However, the emissivity of flames which contain particles of large size parameters deviates considerably from those containing Rayleigh particles. In addition, this study extends the classical radiation measuring techniques, usually used to estimate temperature and concentration of flames having non-interacting Rayleigh particles, to include interaction effects and size parameters larger than Rayleigh limit. Also, a proposed measuring technique which requires two radiation measurements, instead of three required by the classical methods, is presented. In terms of this proposed method, expressions which predict the flame temperature and its soot concentration have been derived.

REFERENCES

1. Y. S. Najjar, Engineering prediction of soot concentration in the primary zone of the gas turbine, *Fuel J.* **64,** 93–98 (1985).
2. R. H. Tourin, *Spectroscopic Gas Temperature Measurement.* Elsevier, Amsterdam (1966).
3. C. F. Bohren and D. R. Huffman, *Absorption and Scattering of Light by Small Particles.* Wiley, New York (1983).
4. M. Born and E. Wolf, *Principles of Optics* (6th Edn). Pergamon Press, Oxford (1986).
5. H. C. Hottel and A. F. Sarofim, *Radiative Transfer,* Chap. 12. McGraw-Hill, New York (1967).
6. R. B. Penndorf, Scattering and extinction coefficients for small absorbing and nonabsorbing aerosols, *J. Opt. Soc. Am.* **52,** 896–904 (1962).
7. M. A. Al-Nimr and V. S. Arpaci, Radiative properties of interacting particles, *J. Heat Transfer* **114,** 950–957 (1992).
8. S. Kumar and C. L. Tien, Dependent absorption and extinction of radiation by small particles, *J. Heat Transfer* **112,** 178–185 (1990).
9. A. Selamet and V. S. Arpaci, Rayleigh limit-Penndorf extension, *Int. J. Heat Mass Transfer* **32,** 1809–1820 (1989).
10. I. S. Gradshteyn and I. M. Ryzhik, *Table of Integrals, Series and Products* (6th Edn), p. 325. Academic Press, London (1980).
11. W. A. Gray and R. Muller, *Engineering Calculations in Radiative Heat Transfer.* Pergamon Press, Oxford (1974).
12. R. Siegel and J. R. Howell, *Thermal Radiation Heat Transfer* (2nd Edn). Hemisphere, Washington; McGraw-Hill, New York (1981).